


$\psi(2S)$ Suppression in Pb-Pb Collisions at the LHCS. Acharya *et al.**
(ALICE Collaboration) (Received 22 December 2022; revised 25 May 2023; accepted 20 November 2023; published 24 January 2024)

The production of the $\psi(2S)$ charmonium state was measured with ALICE in Pb-Pb collisions at $\sqrt{s_{NN}} = 5.02$ TeV, in the dimuon decay channel. A significant signal was observed for the first time at LHC energies down to zero transverse momentum, at forward rapidity ($2.5 < y < 4$). The measurement of the ratio of the inclusive production cross sections of the $\psi(2S)$ and J/ψ resonances is reported as a function of the centrality of the collisions and of transverse momentum, in the region $p_T < 12$ GeV/ c . The results are compared with the corresponding measurements in pp collisions, by forming the double ratio $[\sigma^{\psi(2S)}/\sigma^{J/\psi}]_{\text{Pb-Pb}}/[\sigma^{\psi(2S)}/\sigma^{J/\psi}]_{pp}$. It is found that in Pb-Pb collisions the $\psi(2S)$ is suppressed by a factor of ~ 2 with respect to the J/ψ . The $\psi(2S)$ nuclear modification factor R_{AA} was also obtained as a function of both centrality and p_T . The results show that the $\psi(2S)$ resonance yield is strongly suppressed in Pb-Pb collisions, by a factor of up to ~ 3 with respect to pp . Comparisons of cross section ratios with previous Super Proton Synchrotron findings by the NA50 experiment and of R_{AA} with higher- p_T results at LHC energy are also reported. These results and the corresponding comparisons with calculations of transport and statistical models address questions on the presence and properties of charmonium states in the quark-gluon plasma formed in nuclear collisions at the LHC.

DOI: [10.1103/PhysRevLett.132.042301](https://doi.org/10.1103/PhysRevLett.132.042301)

Quarkonia, the bound states of a heavy quark-antiquark pair, represent an important test bench for quantum chromodynamics (QCD), the theory of strong interactions [1]. The production process of the pair is governed by the hard scale corresponding to the quark mass and occurs on a very short time (~ 0.1 fm/ c), while its binding is a soft process, characterized by timescales that can be an order of magnitude larger [2,3]. Static properties of quarkonia, and, in particular, their complex spectroscopy, can be reproduced by formulating QCD on a discrete lattice in space and time [4]. The quarkonium states can also be used as a probe of strongly interacting extended systems, and, in particular, of the quark-gluon plasma (QGP), a state of matter where quarks and gluons are deconfined over distances much larger than the hadronic size (~ 1 fm). In such a state, which can be created by collisions of heavy ions at ultrarelativistic energies, the large density of free color charges leads to a screening of the quark-antiquark binding and to the dissociation of quarkonia [5]. Effects related to a collisional damping of the states can also be present, leading to a loss of correlation in the pair and, consequently, to a modification of the spectral functions in

the QGP [6]. Finally, the QGP created in the collision expands and cools down until it crosses the pseudocritical temperature T_c (of about 157 MeV for a system with zero net baryonic number [7,8]) for the transition to a hadronic phase. Close to this transition, if the initial multiplicity of heavy quark pairs is large, recombination processes, which counterbalance to a certain extent the suppression in the QGP, may become sizable [9,10]; i.e., quarks and antiquarks close in phase space can recombine to form a quarkonium state. These processes may already be effective even in the QGP phase [11].

A further important element in the study of quarkonium production in heavy-ion collisions is their rich variety of states. Restricting the discussion to charmonia, bound states of charm-anticharm quarks, the ground-level J/ψ vector meson and its radial excitation $\psi(2S)$ differ in binding energy by more than a factor of 10 (~ 640 versus ~ 50 MeV, respectively) and by about a factor of 2 in size [12,13]. As a consequence, the dissociation of the charmonium states depends on the temperature of the medium and is expected to occur sequentially, reflecting the increasing values of their binding energies [14]. Also, the recombination processes might, in principle, have different features, with the larger-size charmonium states being produced later in the evolution of the system [15]. Current theoretical approaches for the complex phenomenology of charmonium production in nuclear collisions include transport models [16,17], where dissociation and recombination rates for quarkonium states in the QGP are

*Full author list given at the end of the Letter.

Published by the American Physical Society under the terms of the [Creative Commons Attribution 4.0 International license](https://creativecommons.org/licenses/by/4.0/). Further distribution of this work must maintain attribution to the author(s) and the published article's title, journal citation, and DOI.

calculated taking into account a lattice-QCD-inspired evaluation of the dependence of their spectral properties on the evolving thermodynamic properties of the medium. In the statistical hadronization model (SHMc) [18], charmonia are assumed to be formed at hadronization according to statistical weights and introducing a charm fugacity factor related to charm conservation and determined by the charm production cross section (in the frame of SHMc, it can be more appropriate to use the word “combination” rather than “recombination,” as there is no binding of charmonium states in the QGP phase). The availability of accurate experimental results for various charmonium states represents a crucial input for the evaluation of the theory approaches and ultimately for the understanding of the existence of bound states of heavy quarks in the QGP.

On the experimental side, a suppression of the J/ψ in Pb-Pb collisions was observed by the NA50 experiment at the CERN Super Proton Synchrotron (SPS) [19] (center of mass energy per nucleon-nucleon collision $\sqrt{s_{NN}} = 17.3$ GeV) and subsequently confirmed at the Relativistic Heavy Ion Collider by PHENIX [20] and STAR [21] (Au-Au at $\sqrt{s_{NN}} = 200$ GeV). At the LHC (Pb-Pb at $\sqrt{s_{NN}} = 2.76$ and 5.02 TeV), the ALICE Collaboration has unambiguously demonstrated the existence and role of the recombination processes, by observing at low transverse momentum (p_T), and in central collisions, a smaller suppression compared to lower-energy results [22]. At high p_T , CMS and ATLAS results indicate a strong J/ψ suppression [23,24], reaching a value of ~ 4 for central collisions, where the geometric overlap of the colliding nuclei is maximal. The suppression in Pb-Pb collisions is quantified via the nuclear modification factor R_{AA} , defined as the ratio between the J/ψ yield in Pb-Pb and the product of the corresponding J/ψ cross section in pp collisions times the average nuclear thickness function $\langle T_{AA} \rangle$ [25], a quantity proportional to the number of nucleon-nucleon collisions.

The $\psi(2S)$ measurements are more challenging, due to the ~ 7.5 lower branching ratio to muon pairs with respect to the J/ψ and the ~ 6 times smaller production cross section in pp collisions at LHC energy [26]. The most accurate result until today was obtained by NA50, which measured a decrease of the cross section ratio between $\psi(2S)$ and J/ψ by a factor of ~ 2 , in Pb-Pb collisions at $\sqrt{s_{NN}} = 17.3$ GeV [27], when increasing the collision centrality. Both transport [11,28] and statistical hadronization models [29] were able to reproduce the main features of this result (see, e.g., Fig. 37 in Ref. [30]). More recently, $\psi(2S)$ production was studied by ATLAS [23] and CMS [24,31], measuring the double ratio between the $\psi(2S)$ and J/ψ cross sections in Pb-Pb and pp collisions at $\sqrt{s_{NN}} = 5.02$ TeV. Their analyses, carried out at midrapidity, show in the high- p_T region a strong relative suppression of the $\psi(2S)$ with respect to J/ψ , by a factor of ~ 2 . For a complete characterization of $\psi(2S)$ production

at these energies, an extension of these results toward low p_T , the kinematic region where recombination effects are maximal, is needed. To date, the previous result by ALICE [32] at $\sqrt{s_{NN}} = 2.76$ TeV does not allow a firm conclusion, due to the large uncertainties.

In this Letter, we present results on inclusive $\psi(2S)$ production, obtained by ALICE in Pb-Pb collisions at $\sqrt{s_{NN}} = 5.02$ TeV. The $\psi(2S)$ is studied by means of its decay to muon pairs in the region $2.5 < y < 4$ and down to zero p_T . Measurements of the (double) ratio of production cross sections between the $\psi(2S)$ and J/ψ , as well as of the $\psi(2S)R_{AA}$, are given. The ALICE detector is described extensively in Refs. [33,34]. In particular, muon detection is carried out by a forward spectrometer consisting of a 3 Tm dipole magnet, a system of two hadron absorbers, and five tracking (cathode pad chambers) and two triggering (resistive plate chambers) stations. The minimum-bias (MB) trigger is obtained as a coincidence of signals from the two V0 scintillator arrays ($-3.7 < \eta < -1.7$ and $2.8 < \eta < 5.1$), also used for the rejection of beam-gas interactions and for the determination of the centrality of the collisions (see below).

The data analyzed in this Letter were collected in 2015 and 2018 and correspond to an integrated luminosity $L_{int} \sim 750 \mu\text{b}^{-1}$. The collisions were classified from central to peripheral according to the decreasing energy deposition in the V0 detectors, which can be related to the degree of geometric overlap of the colliding nuclei [25,35]. Events were recorded using a dimuon trigger, given by the coincidence of a MB trigger together with the detection of a pair of particles with opposite charges in the triggering system of the muon spectrometer. The trigger algorithm applies a nonsharp p_T threshold, which has 50% efficiency at 1 GeV/ c and becomes fully efficient ($> 98\%$) for $p_T > 2$ GeV/ c . Selection criteria were applied at the single muon and muon pair levels (see Ref. [36] for details). Opposite-sign dimuons were selected in the rapidity interval $2.5 < y < 4$.

The signal extraction procedure for the $\psi(2S)$ and J/ψ was based on χ^2 minimization fits of the opposite-sign dimuon invariant-mass spectra. The combinatorial background was subtracted with the help of an event mixing procedure, described in detail in Ref. [32]. The resonance signals were described by a double-sided Crystal Ball function or a pseudo-Gaussian with a mass-dependent width [37]. The position of the pole mass of the J/ψ , as well as its width, were kept as free parameters in the fitting procedure. For the $\psi(2S)$, due to the much smaller statistical significance of its signal, its mass was bound to that of the J/ψ , via the mass difference of the two resonances as provided by the Particle Data Group [38], $m_{\psi(2S)} = m_{J/\psi}^{\text{FIT}} + (m_{\psi(2S)}^{\text{PDG}} - m_{J/\psi}^{\text{PDG}})$. The width was also bound to that of the J/ψ , imposing the same ratio of the J/ψ and $\psi(2S)$ widths as the one measured in the data sample of pp collisions at $\sqrt{s} = 13$ TeV [39] or in

Monte Carlo (MC) simulations (see details below). The same data sample, or the MC, was also used to fix the non-Gaussian tails of the resonance mass spectra. The continuum component of the correlated background remaining in the dimuon distributions after mixed-event subtraction and originating mainly from semimuonic decays of pairs of heavy-flavor hadrons was parametrized using various empirical functions. Fits were performed in two invariant mass intervals, $2 < m_{\mu\mu} < 5 \text{ GeV}/c^2$ and $2.2 < m_{\mu\mu} < 4.5 \text{ GeV}/c^2$, roughly centered in the resonance region. The resonance signals were extracted in four p_T classes for the centrality range 0%–90% and in four centrality classes. For the latter series, the selections $p_T < 12 \text{ GeV}/c$ and $0.3 < p_T < 12 \text{ GeV}/c$ were used for the two most central and peripheral classes, respectively, to remove the low- p_T contribution from photoproduction [40] which becomes important for peripheral collisions. For each kinematic and/or centrality selection, the numbers of detected $\psi(2S)$ and J/ψ were obtained by averaging the results of the various fits. For the complete data sample (0%–90%), they amount to 1.3×10^4 and 9.2×10^5 , respectively. All the invariant mass spectra and the results of the corresponding fits are reported as Supplemental Material [41].

The product of acceptance times efficiency ($A \times \epsilon$) has been calculated by means of a MC simulation. The p_T and y distributions for the generated J/ψ were matched to those extracted from data using an iterative procedure as done in Ref. [42], and the same distributions were also used for the $\psi(2S)$. The misalignment of the detection elements as well as the time-dependent status of each electronic channel during the data-taking period were taken into account in the simulation. The resonance signals were embedded into real events in order to properly reproduce the effect of detector occupancy and its variation from one centrality class to another and then reconstructed. The centrality and p_T -integrated $A \times \epsilon$ values, relative to the $2.5 < y < 4$ interval, are 13.5% and 17.3% for J/ψ and $\psi(2S)$, respectively. As a function of p_T and centrality, the $A \times \epsilon$ vary within a factor of ~ 2 and by about 5%, respectively.

The evaluation of the double ratios and the nuclear modification factors requires the measurement of the charmonium cross sections in pp collisions at $\sqrt{s} = 5.02 \text{ TeV}$. Results from Ref. [43] were used for this purpose, by appropriately combining, where necessary, the $\psi(2S)$ cross sections and the ratios $\sigma_{\psi(2S)}/\sigma_{J/\psi}$, in order to match the p_T binning used in this analysis.

The normalization of the yields per event in Pb-Pb collisions is obtained calculating the number of “equivalent” minimum-bias events as the product of the number of dimuon-triggered events ($\sim 4 \times 10^8$) times the inverse of the probability of having a dimuon trigger in a MB event (F), following the procedure described, e.g., in Ref. [44]. For the 0%–90% centrality class, the value of the normalization factor is $F = 13.1 \pm 0.1$. Finally, the $\langle T_{AA} \rangle$ values were

TABLE I. Contributions to the systematic uncertainties (in percentage). In each column, values with an asterisk correspond to the systematic uncertainties correlated as a function of the corresponding variable. The pp reference entry includes a 1.8% luminosity uncertainty.

	Versus centrality	Versus p_T
	$\psi(2S)R_{AA}$	
Signal extraction	16–22	12–25
Tracking effic.	3*	3
Trigger effic.	1.6*	1.5–2
Matching effic.	1*	1
MC input	2*	2
F	0.7*	0.7*
$\langle T_{AA} \rangle$	0.7–2.3	1*
Centrality	0–7	0.3*
pp ref.	4.7*	7.9–11.1
(Double) ratios		
Signal extraction	16–23	12–24
pp ref.	6.7*	5.5–8.8

taken from Ref. [25] for the centrality intervals directly quoted there or by combining their values for the other intervals.

A summary of the systematic uncertainties affecting the calculation of the (double) ratios and $\psi(2S)R_{AA}$ is given in Table I. They were obtained following similar procedures as those adopted for previous charmonium analyses at forward rapidity, that are detailed, e.g., in Refs. [45,46]. For the signal extraction, the systematic uncertainty was calculated as the root mean square of the values of the number of $\psi(2S)$ obtained by combining different fitting ranges, signal, and residual background shapes. In addition, two different normalization ranges of the mixed-event spectra were tested. Fits with a $\chi^2/\text{n.d.f.} > 2.5$ were excluded from the calculation. For the ingredients entering the $A \times \epsilon$ calculation, the systematic uncertainties related to tracking, triggering, and matching of candidate tracks between tracking and triggering detectors were obtained by comparing information obtained in MC and in data, as described in Ref. [46]. The uncertainty due to the generated y and p_T resonance shapes in the MC was estimated as in Ref. [42], taking into account the statistical uncertainty on the measured distributions used for their definition in the iterative procedure and the possible correlations between the distributions in y and p_T . The uncertainty on F was obtained by comparing the results of two different evaluations as discussed in Ref. [44], while for $\langle T_{AA} \rangle$ they were computed by varying the input parameters of the Glauber calculation used for their estimate [25]. For the centrality evaluation, the systematic uncertainty was obtained varying by $\pm 1\%$ the value of the V0 signal amplitude corresponding to the most central 90% of the hadronic Pb-Pb cross section and reextracting the resonance signal under this

hypothesis, as detailed in Ref. [45]. For the pp reference, uncertainties were obtained by combining the corresponding values from the narrower p_T intervals reported in Ref. [43]. A further uncertainty related to the evaluation of the pp luminosity is also considered in the R_{AA} evaluation [43]. All the uncertainties discussed in this paragraph are added in quadrature to obtain the total systematic uncertainty.

When the $\psi(2S)$ to J/ψ cross section ratios are computed, all uncertainties cancel out except the one related to the signal extraction which is dominated by the former resonance. For the double ratios, the uncertainties on the pp cross section ratio between $\psi(2S)$ and J/ψ were also obtained starting from Ref. [43]. All the results shown in this Letter and the corresponding model calculations refer to inclusive quarkonium production, which includes non-prompt quarkonia, originating from the decay of b hadrons.

In Fig. 1, the ratio of $\psi(2S)$ and J/ψ cross sections (not corrected for the branching ratios of the dimuon decay) is shown as a function of centrality, expressed as the average number of participant nucleons $\langle N_{part} \rangle$. In the lower panel, the values of the double ratio can be read, showing a $\psi(2S)$ suppression, with respect to J/ψ , by a factor of about 2 from pp to Pb-Pb. No significant centrality dependence of

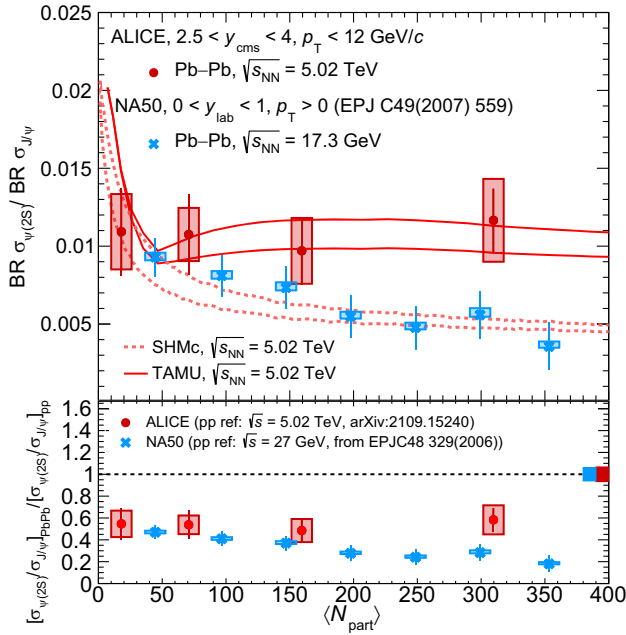


FIG. 1. Ratio of the $\psi(2S)$ and J/ψ inclusive cross sections, not corrected for the corresponding branching ratios (BR) of the dimuon decay, as a function of $\langle N_{part} \rangle$. The vertical error bars and the filled boxes represent statistical and systematic uncertainties, respectively. Data are compared to predictions of the TAMU [15] and SHMc [18,47] models, the corresponding lines showing their uncertainty band, and to results of the SPS NA50 experiment [27]. In the lower panel, the ratios are normalized to the corresponding pp value (double ratio). The filled boxes around the line at unity indicate the global systematic uncertainties.

the results is seen, within the uncertainties. Comparison with calculations of a transport approach (TAMU) [15] and of the SHMc model [18,47] are also shown. The TAMU model reproduces the cross section ratios over centrality, while the SHMc model tends to underestimate the data in central Pb-Pb collisions. The ALICE results are also compared with the corresponding inclusive (double) ratios obtained by NA50 in $0 < y < 1$ [27], which reach smaller values for central events.

In Fig. 2, the nuclear modification factors for $\psi(2S)$ (this analysis) and J/ψ (from Ref. [45]) are compared, as a function of $\langle N_{part} \rangle$. With the limited number of centrality intervals that could be defined, the R_{AA} values for the $\psi(2S)$ do not show a clear trend and are generally consistent with an R_{AA} value of about 0.4. In Fig. 2, calculations with the TAMU model are also shown, indicating a good agreement with the measured R_{AA} for both J/ψ and $\psi(2S)$. The SHMc model reproduces, within uncertainties, the $J/\psi R_{AA}$ centrality dependence, while it underestimates the $\psi(2S)$ production in central and semi-central collisions.

Figure 3 shows the $\psi(2S)R_{AA}$, compared with the corresponding result for the J/ψ [46], as a function of p_T . The corresponding CMS measurements [48] in the region $|y| < 1.6$ and $6.5 < p_T < 30$ GeV/c are also reported. The main feature is an increase of the nuclear modification factor at low p_T , similar to what was observed for the J/ψ and understood as a direct consequence of the recombination process of charm and anticharm quarks. The strong suppression of the $\psi(2S)$ ($R_{AA} \sim 0.15$ at $p_T = 10$ GeV/c) persists up to $p_T = 30$ GeV/c as shown by the CMS data, that agree within uncertainties with those of ALICE in the common p_T range, in spite of the different rapidity coverage. A comparison with predictions from the TAMU model [15] is shown, indicating that also the p_T

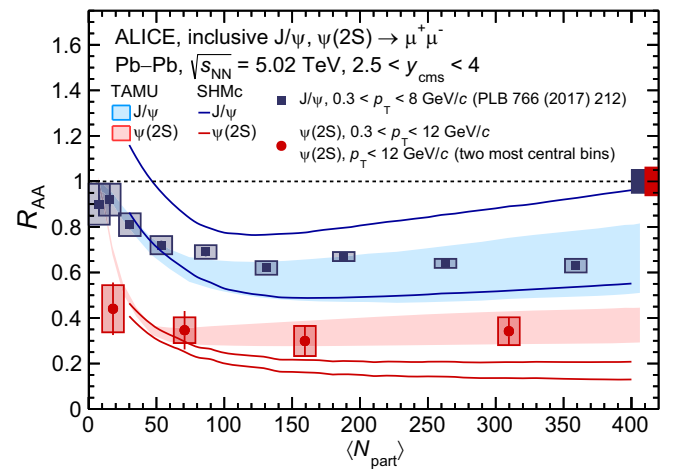


FIG. 2. The R_{AA} for the $\psi(2S)$ (this analysis) and J/ψ [45] as a function of $\langle N_{part} \rangle$. Comparisons with models are also shown, the lines (band) showing the theory uncertainty for the SHMc (transport) calculations.

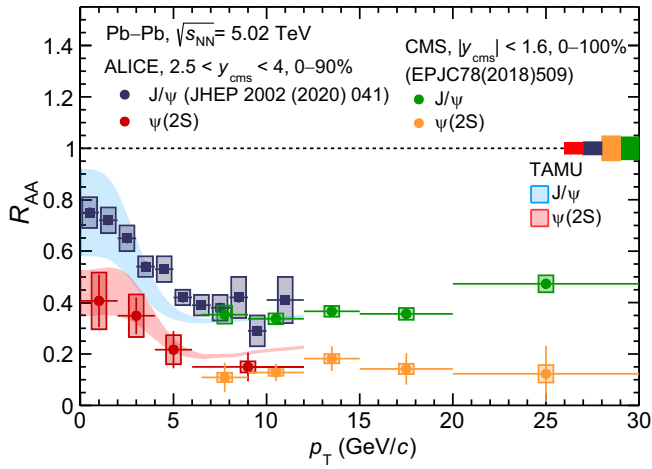


FIG. 3. The R_{AA} for $\psi(2S)$ and J/ψ [45] as a function of p_T . Comparison with theory models and results from the CMS experiment [31] are also shown.

dependence of the R_{AA} is well reproduced for both J/ψ and $\psi(2S)$, as was the case for the centrality dependence. For completeness, we include in Supplemental Material [41] a plot with the (double) ratio of the $\psi(2S)$ cross sections as a function of p_T .

The contribution of nonprompt quarkonia, originating from the decay of b hadrons, could be estimated knowing the fraction F_B of nonprompt charmonia in pp collisions and their R_{AA} in Pb-Pb collisions. An approximate estimate can be carried out using F_B values from LHCb [49,50] and the R_{AA} of nonprompt D mesons measured by ALICE [51] and used as a proxy for nonprompt quarkonia. It shows that prompt J/ψ and $\psi(2S)$ R_{AA} would be smaller by less than 1σ with respect to their inclusive values. However, it should be noted that the input quantities for this evaluation do not precisely correspond to the same kinematic or collision energy region of our data.

The picture emerging from these results shows a clear hierarchy of suppression of J/ψ and $\psi(2S)$ over the whole p_T and centrality intervals explored. Apart from the overall larger $\psi(2S)$ suppression, visible in the double ratios and in the comparison of the R_{AA} , no significant difference in the p_T and centrality dependence of the suppression effects between the two states can be seen. The comparison with SPS results shows that the relative suppression of $\psi(2S)$ with respect to J/ψ in central Pb-Pb events tends to be stronger at low collision energy compared to LHC. However, part of this effect could be due to the different size of the nonprompt component, almost negligible at low energy. When comparing the results with the predictions of statistical and transport models, a significantly better agreement is obtained with the latter, in particular, for central events, as visible in Figs. 1 and 2. We underline that the data-model comparisons are consistently done for inclusive production. The results shown in this Letter favor the scenario where bound states are dissociated or

recombined in the QGP phase, according to the modification of their spectral properties expected from lattice QCD.

In summary, we have provided first accurate results on $\psi(2S)$ production in Pb-Pb collisions at LHC energy down to zero p_T , in the rapidity region $2.5 < y < 4$. Measurements of the cross section ratios between $\psi(2S)$ and J/ψ , of the double ratio between Pb-Pb and pp collisions, and of the nuclear modification factors were shown. A relative suppression by a factor of ~ 2 of the $\psi(2S)$ with respect to the J/ψ is observed, with no significant centrality dependence within the uncertainties. The R_{AA} values for the $\psi(2S)$ show a hint for a decrease as a function of p_T , reminiscent of the same effect observed for the J/ψ and connected with charm quark recombination processes. As a function of centrality, values around $R_{AA} \sim 0.4$ are observed. The theory comparisons show a good agreement with the predictions of the transport model, that include recombination of charm quarks in the QGP phase, while the SHMc model tends to underestimate the data in central Pb-Pb collisions.

The ALICE Collaboration thanks all its engineers and technicians for their invaluable contributions to the construction of the experiment and the CERN accelerator teams for the outstanding performance of the LHC complex. The ALICE Collaboration gratefully acknowledges the resources and support provided by all Grid centers and the Worldwide LHC Computing Grid (WLCG) Collaboration. The ALICE Collaboration acknowledges the following funding agencies for their support in building and running the ALICE detector: A. I. Alikhanyan National Science Laboratory (Yerevan Physics Institute) Foundation (ANSL), State Committee of Science, and World Federation of Scientists (WFS), Armenia; Austrian Academy of Sciences, Austrian Science Fund (FWF): [M 2467-N36], and Nationalstiftung für Forschung, Technologie und Entwicklung, Austria; Ministry of Communications and High Technologies, National Nuclear Research Center, Azerbaijan; Conselho Nacional de Desenvolvimento Científico e Tecnológico (CNPq), Financiadora de Estudos e Projetos (Finep), Fundação de Amparo à Pesquisa do Estado de São Paulo (FAPESP), and Universidade Federal do Rio Grande do Sul (UFRGS), Brazil; Bulgarian Ministry of Education and Science, within the National Roadmap for Research Infrastructures 2020–2027 (object CERN), Bulgaria; Ministry of Education of China (MOEC), Ministry of Science & Technology of China (MSTC), and National Natural Science Foundation of China (NSFC), China; Ministry of Science and Education and Croatian Science Foundation, Croatia; Centro de Aplicaciones Tecnológicas y Desarrollo Nuclear (CEADEN), Cubaenergía, Cuba; Ministry of Education, Youth and Sports of the Czech Republic, Czech Republic; The Danish Council for Independent Research—Natural Sciences, the VILLUM

FONDEN, and Danish National Research Foundation (DNRF), Denmark; Helsinki Institute of Physics (HIP), Finland; Commissariat à l’Energie Atomique (CEA) and Institut National de Physique Nucléaire et de Physique des Particules (IN2P3) and Centre National de la Recherche Scientifique (CNRS), France; Bundesministerium für Bildung und Forschung (BMBF) and GSI Helmholtzzentrum für Schwerionenforschung GmbH, Germany; General Secretariat for Research and Technology, Ministry of Education, Research and Religions, Greece; National Research, Development and Innovation Office, Hungary; Department of Atomic Energy Government of India (DAE), Department of Science and Technology, Government of India (DST), University Grants Commission, Government of India (UGC), and Council of Scientific and Industrial Research (CSIR), India; National Research and Innovation Agency—BRIN, Indonesia; Istituto Nazionale di Fisica Nucleare (INFN), Italy; Japanese Ministry of Education, Culture, Sports, Science and Technology (MEXT) and Japan Society for the Promotion of Science (JSPS) KAKENHI, Japan; Consejo Nacional de Ciencia (CONACYT) y Tecnología, through Fondo de Cooperación Internacional en Ciencia y Tecnología (FONCICYT) and Dirección General de Asuntos del Personal Académico (DGAPA), Mexico; Nederlandse Organisatie voor Wetenschappelijk Onderzoek (NWO), Netherlands; The Research Council of Norway, Norway; Commission on Science and Technology for Sustainable Development in the South (COMSATS), Pakistan; Pontificia Universidad Católica del Perú, Peru; Ministry of Education and Science, National Science Centre, and WUT ID-UB, Poland; Korea Institute of Science and Technology Information and National Research Foundation of Korea (NRF), Republic of Korea; Ministry of Education and Scientific Research, Institute of Atomic Physics, Ministry of Research and Innovation, and Institute of Atomic Physics and University Politehnica of Bucharest, Romania; Ministry of Education, Science, Research and Sport of the Slovak Republic, Slovakia; National Research Foundation of South Africa, South Africa; Swedish Research Council (VR) and Knut & Alice Wallenberg Foundation (KAW), Sweden; European Organization for Nuclear Research, Switzerland; Suranaree University of Technology (SUT), National Science and Technology Development Agency (NSTDA), Thailand Science Research and Innovation (TSRI), and National Science, Research and Innovation Fund (NSRF), Thailand; Turkish Energy, Nuclear and Mineral Research Agency (TENMAK), Turkey; National Academy of Sciences of Ukraine, Ukraine; Science and Technology Facilities Council (STFC), United Kingdom; and National Science Foundation of the United States of America (NSF) and United States Department of Energy, Office of Nuclear Physics (DOE NP), United States of America. In addition, individual groups or members have received support from:

Marie Skłodowska Curie, European Research Council, Strong 2020—Horizon 2020 (Grants No. 950692, No. 824093, and No. 896850), European Union; Academy of Finland (Center of Excellence in Quark Matter) (Grants No. 346327 and No. 346328), Finland; and Programa de Apoyos para la Superación del Personal Académico, UNAM, Mexico.

-
- [1] N. Brambilla *et al.*, Heavy quarkonium: Progress, puzzles, and opportunities, *Eur. Phys. J. C* **71**, 1534 (2011).
 - [2] D. Kharzeev and R. L. Thews, Quarkonium formation time in a model independent approach, *Phys. Rev. C* **60**, 041901 (R) (1999).
 - [3] J. Hufner, Y. P. Ivanov, B. Z. Kopeliovich, and A. V. Tarasov, Photoproduction of charmonia and total charmonium-proton cross sections, *Phys. Rev. D* **62**, 094022 (2000).
 - [4] C. T. H. Davies *et al.* (HPQCD, UKQCD, MILC, and Fermilab Lattice Collaboration), High precision lattice QCD confronts experiment, *Phys. Rev. Lett.* **92**, 022001 (2004).
 - [5] T. Matsui and H. Satz, J/ψ suppression by quark-gluon plasma formation, *Phys. Lett. B* **178**, 416 (1986).
 - [6] M. Laine, O. Philipsen, P. Romatschke, and M. Tassler, Real-time static potential in hot QCD, *J. High Energy Phys.* **03** (2007) 054.
 - [7] A. Bazavov *et al.* (HotQCD Collaboration), Chiral crossover in QCD at zero and non-zero chemical potentials, *Phys. Lett. B* **795**, 15 (2019).
 - [8] S. Borsanyi, Z. Fodor, J. N. Guenther, R. Kara, S. D. Katz, P. Parotto, A. Pasztor, C. Ratti, and K. K. Szabo, QCD crossover at finite chemical potential from lattice simulations, *Phys. Rev. Lett.* **125**, 052001 (2020).
 - [9] P. Braun-Munzinger and J. Stachel, (Non)thermal aspects of charmonium production and a new look at J/ψ suppression, *Phys. Lett. B* **490**, 196 (2000).
 - [10] R. L. Thews, M. Schroedter, and J. Rafelski, Enhanced J/ψ production in deconfined quark matter, *Phys. Rev. C* **63**, 054905 (2001).
 - [11] L. Grandchamp, R. Rapp, and G. E. Brown, In medium effects on charmonium production in heavy ion collisions, *Phys. Rev. Lett.* **92**, 212301 (2004).
 - [12] F. Karsch and H. Satz, The spectral analysis of strongly interacting matter, *Z. Phys. C* **51**, 209 (1991).
 - [13] H. Satz, Colour deconfinement and quarkonium binding, *J. Phys. G* **32**, R25 (2006).
 - [14] S. Digal, P. Petreczky, and H. Satz, Quarkonium feed down and sequential suppression, *Phys. Rev. D* **64**, 094015 (2001).
 - [15] X. Du and R. Rapp, Sequential regeneration of charmonia in heavy-ion collisions, *Nucl. Phys.* **A943**, 147 (2015).
 - [16] X. Zhao and R. Rapp, Medium modifications and production of charmonia at LHC, *Nucl. Phys.* **A859**, 114 (2011).
 - [17] K. Zhou, N. Xu, Z. Xu, and P. Zhuang, Medium effects on charmonium production at ultrarelativistic energies available at the CERN Large Hadron Collider, *Phys. Rev. C* **89**, 054911 (2014).

- [18] A. Andronic, P. Braun-Munzinger, M. K. Köhler, K. Redlich, and J. Stachel, Transverse momentum distributions of charmonium states with the statistical hadronization model, *Phys. Lett. B* **797**, 134836 (2019).
- [19] B. Alessandro *et al.* (NA50 Collaboration), A new measurement of J/ψ suppression in Pb-Pb collisions at 158 GeV per nucleon, *Eur. Phys. J. C* **39**, 335 (2005).
- [20] A. Adare *et al.* (PHENIX Collaboration), J/ψ suppression at forward rapidity in Au + Au collisions at $\sqrt{s_{NN}} = 200$ GeV, *Phys. Rev. C* **84**, 054912 (2011).
- [21] J. Adam *et al.* (STAR Collaboration), Measurement of inclusive J/ψ suppression in Au + Au collisions at $\sqrt{s_{NN}} = 200$ GeV through the dimuon channel at STAR, *Phys. Lett. B* **797**, 134917 (2019).
- [22] S. Acharya *et al.* (ALICE Collaboration), Centrality and transverse momentum dependence of inclusive J/ψ production at midrapidity in Pb-Pb collisions at $\sqrt{s_{NN}} = 5.02$ TeV, *Phys. Lett. B* **805**, 135434 (2020).
- [23] M. Aaboud *et al.* (ATLAS Collaboration), Prompt and non-prompt J/ψ and $\psi(2S)$ suppression at high transverse momentum in 5.02 TeV Pb + Pb collisions with the ATLAS experiment, *Eur. Phys. J. C* **78**, 762 (2018).
- [24] A. M. Sirunyan *et al.* (CMS Collaboration), Relative modification of prompt $\psi(2S)$ and J/ψ yields from pp to PbPb collisions at $\sqrt{s_{NN}} = 5.02$ TeV, *Phys. Rev. Lett.* **118**, 162301 (2017).
- [25] ALICE Collaboration, Centrality determination in heavy ion collisions, Report No. ALICE-PUBLIC-2018-011, CERN, <http://cds.cern.ch/record/2636623>.
- [26] B. Abelev *et al.* (ALICE Collaboration), Measurement of quarkonium production at forward rapidity in pp collisions at $\sqrt{s} = 7$ TeV, *Eur. Phys. J. C* **74**, 2974 (2014).
- [27] B. Alessandro *et al.* (NA50 Collaboration), ψ' production in Pb-Pb collisions at 158 GeV/nucleon, *Eur. Phys. J. C* **49**, 559 (2007).
- [28] L. Grandchamp, R. Rapp, and G. E. Brown, Medium modifications of charm and charmonium in high-energy heavy ion collisions, *J. Phys. G* **30**, S1355 (2004).
- [29] A. Andronic, P. Braun-Munzinger, K. Redlich, and J. Stachel, Statistical hadronization of heavy quarks in ultra-relativistic nucleus-nucleus collisions, *Nucl. Phys.* **A789**, 334 (2007).
- [30] R. Rapp and H. van Hees, Heavy quarks in the quark-gluon plasma, in *Quark-Gluon Plasma 4* (World Scientific, Singapore, 2010), pp. 111–206.
- [31] A. M. Sirunyan *et al.* (CMS Collaboration), Measurement of prompt and nonprompt charmonium suppression in PbPb collisions at 5.02 TeV, *Eur. Phys. J. C* **78**, 509 (2018).
- [32] J. Adam *et al.* (ALICE Collaboration), Differential studies of inclusive J/ψ and $\psi(2S)$ production at forward rapidity in Pb-Pb collisions at $\sqrt{s_{NN}} = 2.76$ TeV, *J. High Energy Phys.* **05** (2016) 179.
- [33] K. Aamodt *et al.* (ALICE Collaboration), The ALICE experiment at the CERN LHC, *J. Instrum.* **3**, S08002 (2008).
- [34] B. Abelev *et al.* (ALICE Collaboration), Performance of the ALICE experiment at the CERN LHC, *Int. J. Mod. Phys. A* **29**, 1430044 (2014).
- [35] B. Abelev *et al.* (ALICE Collaboration), Centrality determination of Pb-Pb collisions at $\sqrt{s_{NN}} = 2.76$ TeV with ALICE, *Phys. Rev. C* **88**, 044909 (2013).
- [36] S. Acharya *et al.* (ALICE Collaboration), Study of J/ψ azimuthal anisotropy at forward rapidity in Pb-Pb collisions at $\sqrt{s_{NN}} = 5.02$ TeV, *J. High Energy Phys.* **02** (2019) 012.
- [37] J. Adam *et al.* (ALICE Collaboration), Quarkonium signal extraction in ALICE, Report No. ALICE-PUBLIC-2015-006, CERN, <https://cds.cern.ch/record/2060096>.
- [38] R. L. Workman *et al.* (Particle Data Group), Review of particle physics, *Prog. Theor. Exp. Phys.* **2022**, 083C01 (2022).
- [39] S. Acharya *et al.* (ALICE Collaboration), Energy dependence of forward-rapidity J/ψ and $\psi(2S)$ production in pp collisions at the LHC, *Eur. Phys. J. C* **77**, 392 (2017).
- [40] ALICE Collaboration, Photoproduction of low- p_T J/ψ from peripheral to central Pb-Pb collisions at 5.02 TeV, *Phys. Lett. B* **846**, 137467 (2023).
- [41] See Supplemental Material at <http://link.aps.org/supplemental/10.1103/PhysRevLett.132.042301> for additional plots of invariant mass spectra and for the additional result on the (double) $\psi(2S)/J/\psi$ cross sections ratio versus transverse momentum.
- [42] S. Acharya *et al.* (ALICE Collaboration), Inclusive J/ψ production at forward and backward rapidity in p-Pb collisions at $\sqrt{s_{NN}} = 8.16$ TeV, *J. High Energy Phys.* **07** (2018) 160.
- [43] S. Acharya *et al.* (ALICE Collaboration), Inclusive quarkonium production in pp collisions at $\sqrt{s} = 5.02$ TeV, *Eur. Phys. J. C* **83**, 61 (2023).
- [44] S. Acharya *et al.* (ALICE Collaboration), Z-boson production in p-Pb collisions at $\sqrt{s_{NN}} = 8.16$ TeV and Pb-Pb collisions at $\sqrt{s_{NN}} = 5.02$ TeV, *J. High Energy Phys.* **09** (2020) 076.
- [45] J. Adam *et al.* (ALICE Collaboration), J/ψ suppression at forward rapidity in Pb-Pb collisions at $\sqrt{s_{NN}} = 5.02$ TeV, *Phys. Lett. B* **766**, 212 (2017).
- [46] S. Acharya *et al.* (ALICE Collaboration), Studies of J/ψ production at forward rapidity in Pb-Pb collisions at $\sqrt{s_{NN}} = 5.02$ TeV, *J. High Energy Phys.* **02** (2020) 041.
- [47] A. Andronic, P. Braun-Munzinger, K. Redlich, and J. Stachel, Decoding the phase structure of QCD via particle production at high energy, *Nature (London)* **561**, 321 (2018).
- [48] A. M. Sirunyan *et al.* (CMS Collaboration), Measurement of prompt and nonprompt charmonium suppression in PbPb collisions at 5.02 TeV, *Eur. Phys. J. C* **78**, 509 (2018).
- [49] R. Aaij *et al.* (LHCb Collaboration), Measurement of $\psi(2S)$ meson production in pp collisions at $\sqrt{s} = 7$ TeV, *Eur. Phys. J. C* **72**, 2100 (2012); **80**, 49(E) (2020).
- [50] R. Aaij *et al.* (LHCb Collaboration), Measurement of J/ψ production cross-sections in pp collisions at $\sqrt{s} = 5$ TeV, *J. High Energy Phys.* **11** (2021) 181.
- [51] S. Acharya *et al.* (ALICE Collaboration), Measurement of beauty production via non-prompt D^0 mesons in Pb-Pb collisions at $\sqrt{s_{NN}} = 5.02$ TeV, *J. High Energy Phys.* **12** (2022) 126.

S. Acharya,¹²⁵ D. Adamová,⁸⁶ A. Adler,⁶⁹ G. Aglieri Rinella,³² M. Agnello,²⁹ N. Agrawal,⁵⁰ Z. Ahammed,¹³² S. Ahmad,¹⁵
 S. U. Ahn,⁷⁰ I. Ahuja,³⁷ A. Akindinov,¹⁴⁰ M. Al-Turany,⁹⁷ D. Aleksandrov,¹⁴⁰ B. Alessandro,⁵⁵ H. M. Alfanda,⁶
 R. Alfaro Molina,⁶⁶ B. Ali,¹⁵ A. Alici,²⁵ N. Alizadehvandchali,¹¹⁴ A. Alkin,³² J. Alme,²⁰ G. Alocco,⁵¹ T. Alt,⁶³
 I. Altsybeev,¹⁴⁰ M. N. Anaam,⁶ C. Andrei,⁴⁵ A. Andronic,¹³⁵ V. Anguelov,⁹⁴ F. Antinori,⁵³ P. Antonioli,⁵⁰ N. Apadula,⁷⁴
 L. Aphecetche,¹⁰³ H. Appelshäuser,⁶³ C. Arata,⁷³ S. Arcelli,²⁵ M. Aresti,⁵¹ R. Arnaldi,⁵⁵ I. C. Arsene,¹⁹ M. Arslandok,¹³⁷
 A. Augustinus,³² R. Averbeck,⁹⁷ M. D. Azmi,¹⁵ A. Badalà,⁵² J. Bae,¹⁰⁴ Y. W. Baek,⁴⁰ X. Bai,¹¹⁸ R. Bailhache,⁶³ Y. Bailung,⁴⁷
 A. Balbino,²⁹ A. Baldisseri,¹²⁸ B. Balis,² D. Banerjee,⁴ Z. Banoo,⁹¹ R. Barbera,²⁶ F. Barile,³¹ L. Barioglio,⁹⁵ M. Barlou,⁷⁸
 G. G. Barnaföldi,¹³⁶ L. S. Barnby,⁸⁵ V. Barret,¹²⁵ L. Barreto,¹¹⁰ C. Bartels,¹¹⁷ K. Barth,³² E. Bartsch,⁶³ F. Baruffaldi,²⁷
 N. Bastid,¹²⁵ S. Basu,⁷⁵ G. Batigne,¹⁰³ D. Battistini,⁹⁵ B. Batyunya,¹⁴¹ D. Bauri,⁴⁶ J. L. Bazo Alba,¹⁰¹ I. G. Bearden,⁸³
 C. Beattie,¹³⁷ P. Becht,⁹⁷ D. Behera,⁴⁷ I. Belikov,¹²⁷ A. D. C. Bell Hechavarria,¹³⁵ F. Bellini,²⁵ R. Bellwied,¹¹⁴
 S. Belokurova,¹⁴⁰ V. Belyaev,¹⁴⁰ G. Bencedi,¹³⁶ S. Beole,²⁴ A. Bercuci,⁴⁵ Y. Berdnikov,¹⁴⁰ A. Berdnikova,⁹⁴ L. Bergmann,⁹⁴
 M. G. Besoiu,⁶² L. Betev,³² P. P. Bhaduri,¹³² A. Bhasin,⁹¹ M. A. Bhat,⁴ B. Bhattacharjee,⁴¹ L. Bianchi,²⁴ N. Bianchi,⁴⁸
 J. Bielčik,³⁵ J. Bielčiková,⁸⁶ J. Biernat,¹⁰⁷ A. P. Bigot,¹²⁷ A. Bilandzic,⁹⁵ G. Biro,¹³⁶ S. Biswas,⁴ N. Bize,¹⁰³ J. T. Blair,¹⁰⁸
 D. Blau,¹⁴⁰ M. B. Blidaru,⁹⁷ N. Bluhme,³⁸ C. Blume,⁶³ G. Boca,^{21,54} F. Bock,⁸⁷ T. Bodova,²⁰ A. Bogdanov,¹⁴⁰ S. Boi,²²
 J. Bok,⁵⁷ L. Boldizsár,¹³⁶ A. Bolozdynya,¹⁴⁰ M. Bombara,³⁷ P. M. Bond,³² G. Bonomi,^{54,131} H. Borel,¹²⁸ A. Borissov,¹⁴⁰
 A. G. Borquez Carcamo,⁹⁴ H. Bossi,¹³⁷ E. Botta,²⁴ Y. E. M. Bouziani,⁶³ L. Bratrud,⁶³ P. Braun-Munzinger,⁹⁷ M. Bregant,¹¹⁰
 M. Broz,³⁵ G. E. Bruno,^{31,96} D. Budnikov,¹⁴⁰ H. Buesching,⁶³ S. Bufalino,²⁹ O. Bugnon,¹⁰³ P. Buhler,¹⁰² Z. Buthelezi,^{67,121}
 S. A. Bysiak,¹⁰⁷ M. Cai,⁶ H. Caines,¹³⁷ A. Caliva,⁹⁷ E. Calvo Villar,¹⁰¹ J. M. M. Camacho,¹⁰⁹ P. Camerini,²³
 F. D. M. Canedo,¹¹⁰ M. Carabas,¹²⁴ A. A. Carballo,³² F. Carnesecchi,³² R. Caron,¹²⁶ J. Castillo Castellanos,¹²⁸
 F. Catalano,^{24,29} C. Ceballos Sanchez,¹⁴¹ I. Chakaberia,⁷⁴ P. Chakraborty,⁴⁶ S. Chandra,¹³² S. Chapeland,³² M. Chartier,¹¹⁷
 S. Chattopadhyay,¹³² S. Chattopadhyay,⁹⁹ T. G. Chavez,⁴⁴ T. Cheng,^{6,97} C. Cheshkov,¹²⁶ B. Cheynis,¹²⁶
 V. Chibante Barroso,³² D. D. Chinellato,¹¹¹ E. S. Chizzali,^{95,b} J. Cho,⁵⁷ S. Cho,⁵⁷ P. Chochula,³² P. Christakoglou,⁸⁴
 C. H. Christensen,⁸³ P. Christiansen,⁷⁵ T. Chujo,¹²³ M. Ciaccio,²⁹ C. Cicalo,⁵¹ F. Cindolo,⁵⁰ M. R. Ciupek,⁹⁷ G. Clai,^{50,c}
 F. Colamaria,⁴⁹ J. S. Colburn,¹⁰⁰ D. Colella,^{31,96} M. Colocci,³² M. Concas,^{55,d} G. Conesa Balbastre,⁷³ Z. Conesa del Valle,⁷²
 G. Contin,²³ J. G. Contreras,³⁵ M. L. Coquet,¹²⁸ T. M. Cormier,^{87,a} P. Cortese,^{55,130} M. R. Cosentino,¹¹² F. Costa,³²
 S. Costanza,^{21,54} J. Crkovská,⁹⁴ P. Crochet,¹²⁵ R. Cruz-Torres,⁷⁴ E. Cuautle,⁶⁴ P. Cui,⁶ A. Dainese,⁵³ M. C. Danisch,⁹⁴
 A. Danu,⁶² P. Das,⁸⁰ P. Das,⁴ S. Das,⁴ A. R. Dash,¹³⁵ S. Dash,⁴⁶ A. De Caro,²⁸ G. de Cataldo,⁴⁹ J. de Cuveland,³⁸
 A. De Falco,²² D. De Gruttola,²⁸ N. De Marco,⁵⁵ C. De Martin,²³ S. De Pasquale,²⁸ S. Deb,⁴⁷ R. J. Debski,² K. R. Deja,¹³³
 R. Del Grande,⁹⁵ L. Dello Stritto,²⁸ W. Deng,⁶ P. Dhankher,¹⁸ D. Di Bari,³¹ A. Di Mauro,³² R. A. Diaz,^{7,141} T. Dietel,¹¹³
 Y. Ding,^{6,126} R. Divià,³² D. U. Dixit,¹⁸ Ø. Djuvsland,²⁰ U. Dmitrieva,¹⁴⁰ A. Dobrin,⁶² B. Dönigus,⁶³ J. M. Dubinski,¹³³
 A. Dubla,⁹⁷ S. Dudi,⁹⁰ P. Dupieux,¹²⁵ M. Durkac,¹⁰⁶ N. Dzalaiova,¹² T. M. Eder,¹³⁵ R. J. Ehlers,⁸⁷ V. N. Eikeland,²⁰
 F. Eisenhut,⁶³ D. Elia,⁴⁹ B. Erazmus,¹⁰³ F. Ercolessi,²⁵ F. Erhardt,⁸⁹ M. R. Ersdal,²⁰ B. Espagnon,⁷² G. Eulisse,³² D. Evans,¹⁰⁰
 S. Evdokimov,¹⁴⁰ L. Fabbietti,⁹⁵ M. Faggin,²⁷ J. Faivre,⁷³ F. Fan,⁶ W. Fan,⁷⁴ A. Fantoni,⁴⁸ M. Fasel,⁸⁷ P. Feccchio,²⁹
 A. Feliciello,⁵⁵ G. Feofilov,¹⁴⁰ A. Fernández Téllez,⁴⁴ L. Ferrandi,¹¹⁰ M. B. Ferrer,³² A. Ferrero,¹²⁸ C. Ferrero,⁵⁵ A. Ferretti,²⁴
 V. J. G. Feuillard,⁹⁴ V. Filova,³⁵ D. Finogeev,¹⁴⁰ F. M. Fionda,⁵¹ F. Flor,¹¹⁴ A. N. Flores,¹⁰⁸ S. Foertsch,⁶⁷ I. Fokin,⁹⁴
 S. Fokin,¹⁴⁰ E. Fragiaco,⁵⁶ E. Frajna,¹³⁶ U. Fuchs,³² N. Funicello,²⁸ C. Furget,⁷³ A. Furs,¹⁴⁰ T. Fusayasu,⁹⁸
 J. J. Gaardhøje,⁸³ M. Gagliardi,²⁴ A. M. Gago,¹⁰¹ C. D. Galvan,¹⁰⁹ D. R. Gangadharan,¹¹⁴ P. Ganoti,⁷⁸ C. Garabatos,⁹⁷
 J. R. A. Garcia,⁴⁴ E. Garcia-Solis,⁹ K. Garg,¹⁰³ C. Gargiulo,³² A. Garibli,⁸¹ K. Garner,¹³⁵ P. Gasik,⁹⁷ A. Gautam,¹¹⁶
 M. B. Gay Ducati,⁶⁵ M. Germain,¹⁰³ C. Ghosh,¹³² M. Giacalone,²⁵ P. Giubellino,^{55,97} P. Giubilato,²⁷ A. M. C. Glaenger,¹²⁸
 P. Glässel,⁹⁴ E. Glimos,¹²⁰ D. J. Q. Goh,⁷⁶ V. Gonzalez,¹³⁴ L. H. González-Trueba,⁶⁶ M. Gorgon,² S. Gotovac,³³
 V. Grabski,⁶⁶ L. K. Graczykowski,¹³³ E. Grecka,⁸⁶ A. Grelli,⁵⁸ C. Grigoras,³² V. Grigoriev,¹⁴⁰ S. Grigoryan,^{1,141} F. Grosa,³²
 J. F. Grosse-Oetringhaus,³² R. Grosso,⁹⁷ D. Grund,³⁵ G. G. Guardiano,¹¹¹ R. Guernane,⁷³ M. Guilbaud,¹⁰³ K. Gulbrandsen,⁸³
 T. Gundem,⁶³ T. Gunji,¹²² W. Guo,⁶ A. Gupta,⁹¹ R. Gupta,⁹¹ S. P. Guzman,⁴⁴ L. Gyulai,¹³⁶ M. K. Habib,⁹⁷ C. Hadjidakis,⁷²
 F. U. Haider,⁹¹ H. Hamagaki,⁷⁶ A. Hamdi,⁷⁴ M. Hamid,⁶ Y. Han,¹³⁸ R. Hannigan,¹⁰⁸ M. R. Haque,¹³³ J. W. Harris,¹³⁷
 A. Harton,⁹ H. Hassan,⁸⁷ D. Hatzifotiadou,⁵⁰ P. Hauer,⁴² L. B. Havener,¹³⁷ S. T. Heckel,⁹⁵ E. Hellbär,⁹⁷ H. Helstrup,³⁴
 M. Hemmer,⁶³ T. Herman,³⁵ G. Herrera Corral,⁸ F. Herrmann,¹³⁵ S. Herrmann,¹²⁶ K. F. Hetland,³⁴ B. Heybeck,⁶³
 H. Hillemanns,³² C. Hills,¹¹⁷ B. Hippolyte,¹²⁷ B. Hofman,⁵⁸ B. Hohlweger,⁸⁴ G. H. Hong,¹³⁸ M. Horst,⁹⁵ A. Horzyk,²

R. Hosokawa,¹⁴ Y. Hou,⁶ P. Hristov,³² C. Hughes,¹²⁰ P. Huhn,⁶³ L. M. Huhta,¹¹⁵ C. V. Hulse,⁷² T. J. Humanic,⁸⁸
H. Hushnud,^{99,15} A. Hutson,¹¹⁴ D. Hutter,³⁸ J. P. Iddon,¹¹⁷ R. Ilkaev,¹⁴⁰ H. Ilyas,¹³ M. Inaba,¹²³ G. M. Innocenti,³²
M. Ippolitov,¹⁴⁰ A. Isakov,⁸⁶ T. Isidori,¹¹⁶ M. S. Islam,⁹⁹ M. Ivanov,¹² M. Ivanov,⁹⁷ V. Ivanov,¹⁴⁰ M. Jablonski,² B. Jacak,⁷⁴
N. Jacazio,³² P. M. Jacobs,⁷⁴ S. Jadlovska,¹⁰⁶ J. Jadlovsky,¹⁰⁶ S. Jaelani,⁸² L. Jaffe,³⁸ C. Jahnke,¹¹¹ M. J. Jakubowska,¹³³
M. A. Janik,¹³³ T. Janson,⁶⁹ M. Jercic,⁸⁹ S. Jia,¹⁰ A. A. P. Jimenez,⁶⁴ F. Jonas,⁸⁷ J. M. Jowett,^{32,97} J. Jung,⁶³ M. Jung,⁶³
A. Junique,³² A. Jusko,¹⁰⁰ M. J. Kabus,^{32,133} J. Kaewjai,¹⁰⁵ P. Kalinak,⁵⁹ A. S. Kalteyer,⁹⁷ A. Kalweit,³² V. Kaplin,¹⁴⁰
A. Karasu Uysal,⁷¹ D. Karatovic,⁸⁹ O. Karavichev,¹⁴⁰ T. Karavicheva,¹⁴⁰ P. Karczmarczyk,¹³³ E. Karpechev,¹⁴⁰
U. Kebschull,⁶⁹ R. Keidel,¹³⁹ D. L. D. Keijdener,⁵⁸ M. Keil,³² B. Ketzer,⁴² A. M. Khan,⁶ S. Khan,¹⁵ A. Khanzadeev,¹⁴⁰
Y. Kharlov,¹⁴⁰ A. Khatun,^{15,116} A. Khuntia,¹⁰⁷ M. B. Kidson,¹¹³ B. Kileng,³⁴ B. Kim,¹⁶ C. Kim,¹⁶ D. J. Kim,¹¹⁵ E. J. Kim,⁶⁸
J. Kim,¹³⁸ J. S. Kim,⁴⁰ J. Kim,⁹⁴ J. Kim,⁶⁸ M. Kim,^{18,94} S. Kim,¹⁷ T. Kim,¹³⁸ K. Kimura,⁹² S. Kirsch,⁶³ I. Kisel,³⁸
S. Kiselev,¹⁴⁰ A. Kisiel,¹³³ J. P. Kitowski,² J. L. Klay,⁵ J. Klein,³² S. Klein,⁷⁴ C. Klein-Bösing,¹³⁵ M. Kleiner,⁶³ T. Klemenz,⁹⁵
A. Kluge,³² A. G. Knospe,¹¹⁴ C. Kobdaj,¹⁰⁵ T. Kollegger,⁹⁷ A. Kondratyev,¹⁴¹ E. Kondratyuk,¹⁴⁰ J. König,⁶³
S. A. Königstorfer,⁹⁵ P. J. Konopka,³² G. Kornakov,¹³³ S. D. Koryciak,² A. Kotliarov,⁸⁶ V. Kovalenko,¹⁴⁰ M. Kowalski,¹⁰⁷
V. Kozhuharov,³⁶ I. Králik,⁵⁹ A. Kravčáková,³⁷ L. Kreis,⁹⁷ M. Krivda,^{59,100} F. Krizek,⁸⁶ K. Krizkova Gajdosova,³⁵
M. Kroesen,⁹⁴ M. Krüger,⁶³ D. M. Krupova,³⁵ E. Kryshen,¹⁴⁰ V. Kučera,³² C. Kuhn,¹²⁷ P. G. Kuijer,⁸⁴ T. Kumaoka,¹²³
D. Kumar,¹³² L. Kumar,⁹⁰ N. Kumar,⁹⁰ S. Kumar,³¹ S. Kundu,³² P. Kurashvili,⁷⁹ A. Kurepin,¹⁴⁰ A. B. Kurepin,¹⁴⁰
A. Kuryakin,¹⁴⁰ S. Kushpil,⁸⁶ J. Kvapil,¹⁰⁰ M. J. Kweon,⁵⁷ J. Y. Kwon,⁵⁷ Y. Kwon,¹³⁸ S. L. La Pointe,³⁸ P. La Rocca,²⁶
Y. S. Lai,⁷⁴ A. Lakrathok,¹⁰⁵ M. Lamanna,³² R. Langoy,¹¹⁹ P. Larionov,³² E. Laudi,³² L. Lautner,^{32,95} R. Lavicka,¹⁰²
T. Lazareva,¹⁴⁰ R. Lea,^{54,131} H. Lee,¹⁰⁴ G. Legras,¹³⁵ J. Lehrbach,³⁸ R. C. Lemmon,⁸⁵ I. León Monzón,¹⁰⁹ M. M. Lesch,⁹⁵
E. D. Lesser,¹⁸ M. Lettrich,⁹⁵ P. Lévai,¹³⁶ X. Li,¹⁰ X. L. Li,⁶ J. Lien,¹¹⁹ R. Lietava,¹⁰⁰ B. Lim,^{16,24} S. H. Lim,¹⁶
V. Lindenstruth,³⁸ A. Lindner,⁴⁵ C. Lippmann,⁹⁷ A. Liu,¹⁸ D. H. Liu,⁶ J. Liu,¹¹⁷ I. M. Lofnes,²⁰ C. Loizides,⁸⁷ S. Lokos,¹⁰⁷
P. Loncar,³³ J. A. Lopez,⁹⁴ X. Lopez,¹²⁵ E. López Torres,⁷ P. Lu,^{97,118} J. R. Luhder,¹³⁵ M. Lunardon,²⁷ G. Luparello,⁵⁶
Y. G. Ma,³⁹ A. Maevskaya,¹⁴⁰ M. Mager,³² T. Mahmoud,⁴² A. Maire,¹²⁷ M. V. Makariev,³⁶ M. Malaev,¹⁴⁰ G. Malfattore,²⁵
N. M. Malik,⁹¹ Q. W. Malik,¹⁹ S. K. Malik,⁹¹ L. Malinina,^{141,g} D. Mal'Kevich,¹⁴⁰ D. Mallick,⁸⁰ N. Mallick,⁴⁷
G. Mandaglio,^{30,52} V. Manko,¹⁴⁰ F. Manso,¹²⁵ V. Manzari,⁴⁹ Y. Mao,⁶ G. V. Margagliotti,²³ A. Margotti,⁵⁰ A. Marín,⁹⁷
C. Markert,¹⁰⁸ P. Martinengo,³² J. L. Martinez,¹¹⁴ M. I. Martínez,⁴⁴ G. Martínez García,¹⁰³ S. Masciocchi,⁹⁷ M. Masera,²⁴
A. Masoni,⁵¹ L. Massacrier,⁷² A. Mastroserio,^{49,129} A. M. Mathis,⁹⁵ O. Matonoha,⁷⁵ P. F. T. Matuoka,¹¹⁰ A. Matyja,¹⁰⁷
C. Mayer,¹⁰⁷ A. L. Mazuecos,³² F. Mazzaschi,²⁴ M. Mazzilli,³² J. E. Mdhluli,¹²¹ A. F. Mechler,⁶³ Y. Melikyan,^{43,140}
A. Menchaca-Rocha,⁶⁶ E. Meninno,^{28,102} A. S. Menon,¹¹⁴ M. Meres,¹² S. Mhlanga,^{67,113} Y. Miake,¹²³ L. Micheletti,⁵⁵
L. C. Migliorin,¹²⁶ D. L. Mihaylov,⁹⁵ K. Mikhaylov,^{140,141} A. N. Mishra,¹³⁶ D. Miśkowiec,⁹⁷ A. Modak,⁴ A. P. Mohanty,⁵⁸
B. Mohanty,⁸⁰ M. Mohisin Khan,^{15,e} M. A. Molander,⁴³ Z. Moravcova,⁸³ C. Mordasini,⁹⁵ D. A. Moreira De Godoy,¹³⁵
I. Morozov,¹⁴⁰ A. Morsch,³² T. Mrnjavac,³² V. Muccifora,⁴⁸ S. Muhuri,¹³² J. D. Mulligan,⁷⁴ A. Mulliri,²² M. G. Munhoz,¹¹⁰
R. H. Munzer,⁶³ H. Murakami,¹²² S. Murray,¹¹³ L. Musa,³² J. Musinsky,⁵⁹ J. W. Myrcha,¹³³ B. Naik,¹²¹ A. I. Nambrath,¹⁸
B. K. Nandi,⁴⁶ R. Nania,⁵⁰ E. Nappi,⁴⁹ A. F. Nassirpour,⁷⁵ A. Nath,⁹⁴ C. Nattrass,¹²⁰ M. N. Naydenov,³⁶ A. Neagu,¹⁹
A. Negru,¹²⁴ L. Nellen,⁶⁴ S. V. Nesbo,³⁴ G. Neskovic,³⁸ D. Nesterov,¹⁴⁰ B. S. Nielsen,⁸³ E. G. Nielsen,⁸³ S. Nikolaev,¹⁴⁰
S. Nikulin,¹⁴⁰ V. Nikulin,¹⁴⁰ F. Noferini,⁵⁰ S. Noh,¹¹ P. Nomokonov,¹⁴¹ J. Norman,¹¹⁷ N. Novitzky,¹²³ P. Nowakowski,¹³³
A. Nyanin,¹⁴⁰ J. Nystrand,²⁰ M. Ogino,⁷⁶ A. Ohlson,⁷⁵ V. A. Okorokov,¹⁴⁰ J. Oleniacz,¹³³ A. C. Oliveira Da Silva,¹²⁰
M. H. Oliver,¹³⁷ A. Onnerstad,¹¹⁵ C. Oppedisano,⁵⁵ A. Ortiz Velasquez,⁶⁴ J. Otwinowski,¹⁰⁷ M. Oya,⁹² K. Oyama,⁷⁶
Y. Pachmayer,⁹⁴ S. Padhan,⁴⁶ D. Pagano,^{54,131} G. Paić,⁶⁴ A. Palasciano,⁴⁹ S. Panebianco,¹²⁸ H. Park,¹²³ H. Park,¹⁰⁴ J. Park,⁵⁷
J. E. Parkkila,³² R. N. Patra,⁹¹ B. Paul,²² H. Pei,⁶ T. Peitzmann,⁵⁸ X. Peng,⁶ M. Pennisi,²⁴ L. G. Pereira,⁶⁵ D. Peresunko,¹⁴⁰
G. M. Perez,⁷ S. Perrin,¹²⁸ Y. Pestov,¹⁴⁰ V. Petráček,³⁵ V. Petrov,¹⁴⁰ M. Petrovici,⁴⁵ R. P. Pezzi,^{65,103} S. Piano,⁵⁶ M. Pikna,¹²
P. Pillot,¹⁰³ O. Pinazza,^{32,50} L. Pinsky,¹¹⁴ C. Pinto,⁹⁵ S. Pisano,⁴⁸ M. Płoskoń,⁷⁴ M. Planinic,⁸⁹ F. Pliquett,⁶³
M. G. Poghosyan,⁸⁷ B. Polichtchouk,¹⁴⁰ S. Politano,²⁹ N. Poljak,⁸⁹ A. Pop,⁴⁵ S. Porteboeuf-Houssais,¹²⁵ V. Pozdniakov,¹⁴¹
K. K. Pradhan,⁴⁷ S. K. Prasad,⁴ S. Prasad,⁴⁷ R. Preghenella,⁵⁰ F. Prino,⁵⁵ C. A. Pruneau,¹³⁴ I. Pshenichnov,¹⁴⁰ M. Puccio,³²
S. Pucillo,²⁴ Z. Pugelova,¹⁰⁶ S. Qiu,⁸⁴ L. Quaglia,²⁴ R. E. Quishpe,¹¹⁴ S. Ragoni,^{14,100} A. Rakotozafindrabe,¹²⁸
L. Ramello,^{55,130} F. Rami,¹²⁷ S. A. R. Ramirez,⁴⁴ T. A. Rancien,⁷³ M. Rasa,²⁶ S. S. Räsänen,⁴³ R. Rath,^{47,50} M. P. Rauch,²⁰
I. Ravasenga,⁸⁴ K. F. Read,^{87,120} C. Reckziegel,¹¹² A. R. Redelbach,³⁸ K. Redlich,^{79,f} A. Rehman,²⁰ F. Reidt,³²
H. A. Reme-Ness,³⁴ Z. Rescakova,³⁷ K. Reygers,⁹⁴ A. Riabov,¹⁴⁰ V. Riabov,¹⁴⁰ R. Ricci,²⁸ M. Richter,¹⁹ A. A. Riedel,⁹⁵
W. Riegler,³² C. Ristea,⁶² M. Rodríguez Cahuantzi,⁴⁴ K. Røed,¹⁹ R. Rogalev,¹⁴⁰ E. Rogochaya,¹⁴¹ T. S. Rogoschinski,⁶³

D. Rohr,³² D. Röhrich,²⁰ P. F. Rojas,⁴⁴ S. Rojas Torres,³⁵ P. S. Rokita,¹³³ G. Romanenko,¹⁴¹ F. Ronchetti,⁴⁸ A. Rosano,^{30,52} E. D. Rosas,⁶⁴ A. Rossi,⁵³ A. Roy,⁴⁷ S. Roy,⁴⁶ N. Rubini,²⁵ O. V. Rueda,^{75,114} D. Ruggiano,¹³³ R. Rui,²³ B. Romyantsev,¹⁴¹ P. G. Russek,² R. Russo,⁸⁴ A. Rustamov,⁸¹ E. Ryabinkin,¹⁴⁰ Y. Ryabov,¹⁴⁰ A. Rybicki,¹⁰⁷ H. Rytönen,¹¹⁵ W. Rzeska,¹³³ O. A. M. Saarimäki,⁴³ R. Sadek,¹⁰³ S. Sadhu,³¹ S. Sadovsky,¹⁴⁰ J. Saetre,²⁰ K. Šafařík,³⁵ S. K. Saha,⁴ S. Saha,⁸⁰ B. Sahoo,⁴⁶ R. Sahoo,⁴⁷ S. Sahoo,⁶⁰ D. Sahu,⁴⁷ P. K. Sahu,⁶⁰ J. Saini,¹³² K. Sajdakova,³⁷ S. Sakai,¹²³ M. P. Salvan,⁹⁷ S. Sambyal,⁹¹ I. Sanna,^{32,95} T. B. Saramela,¹¹⁰ D. Sarkar,¹³⁴ N. Sarkar,¹³² P. Sarma,⁴¹ V. Sarritzu,²² V. M. Sarti,⁹⁵ M. H. P. Sas,¹³⁷ J. Schambach,⁸⁷ H. S. Scheid,⁶³ C. Schiaua,⁴⁵ R. Schicker,⁹⁴ A. Schmah,⁹⁴ C. Schmidt,⁹⁷ H. R. Schmidt,⁹³ M. O. Schmidt,³² M. Schmidt,⁹³ N. V. Schmidt,⁸⁷ A. R. Schmier,¹²⁰ R. Schotter,¹²⁷ A. Schröter,³⁸ J. Schukraft,³² K. Schwarz,⁹⁷ K. Schweda,⁹⁷ G. Scioli,²⁵ E. Scomparin,⁵⁵ J. E. Seger,¹⁴ Y. Sekiguchi,¹²² D. Sekihata,¹²² I. Selyuzhenkov,^{97,140} S. Senyukov,¹²⁷ J. J. Seo,⁵⁷ D. Serebryakov,¹⁴⁰ L. Šerkšnytė,⁹⁵ A. Sevcenco,⁶² T. J. Shaba,⁶⁷ A. Shabetai,¹⁰³ R. Shahoyan,³² A. Shangaraev,¹⁴⁰ A. Sharma,⁹⁰ D. Sharma,⁴⁶ H. Sharma,¹⁰⁷ M. Sharma,⁹¹ S. Sharma,⁷⁶ S. Sharma,⁹¹ U. Sharma,⁹¹ A. Shatat,⁷² O. Sheibani,¹¹⁴ K. Shigaki,⁹² M. Shimomura,⁷⁷ J. Shin,¹¹ S. Shirinkin,¹⁴⁰ Q. Shou,³⁹ Y. Sibirskiy,¹⁴⁰ S. Siddhanta,⁵¹ T. Siemiarczuk,⁷⁹ T. F. Silva,¹¹⁰ D. Silvermyr,⁷⁵ T. Simantathammakul,¹⁰⁵ R. Simeonov,³⁶ B. Singh,⁹¹ B. Singh,⁹⁵ R. Singh,⁸⁰ R. Singh,⁹¹ R. Singh,⁴⁷ S. Singh,¹⁵ V. K. Singh,¹³² V. Singhal,¹³² T. Sinha,⁹⁹ B. Sitar,¹² M. Sitta,^{55,130} T. B. Skaali,¹⁹ G. Skorodumovs,⁹⁴ M. Slupecki,⁴³ N. Smirnov,¹³⁷ R. J. M. Snellings,⁵⁸ E. H. Solheim,¹⁹ J. Song,¹¹⁴ A. Songmoolnak,¹⁰⁵ F. Soramel,²⁷ R. Spijkers,⁸⁴ I. Sputowska,¹⁰⁷ J. Staa,⁷⁵ J. Stachel,⁹⁴ I. Stan,⁶² P. J. Steffanic,¹²⁰ S. F. Stiefelmaier,⁹⁴ D. Stocco,¹⁰³ I. Storehaug,¹⁹ P. Stratmann,¹³⁵ S. Strazzi,²⁵ C. P. Stylianidis,⁸⁴ A. A. P. Suaide,¹¹⁰ C. Suire,⁷² M. Sukhanov,¹⁴⁰ M. Suljic,³² R. Sultanov,¹⁴⁰ V. Sumberia,⁹¹ S. Sumowidagdo,⁸² S. Swain,⁶⁰ I. Szarka,¹² S. F. Taghavi,⁹⁵ G. Tallepied,⁹⁷ J. Takahashi,¹¹¹ G. J. Tambave,²⁰ S. Tang,^{6,125} Z. Tang,¹¹⁸ J. D. Tapia Takaki,¹¹⁶ N. Tapus,¹²⁴ L. A. Tarasovicova,¹³⁵ M. G. Tarzila,⁴⁵ G. F. Tassielli,³¹ A. Tauro,³² G. Tejeda Muñoz,⁴⁴ A. Telesca,³² L. Terlizzi,²⁴ C. Terrevoli,¹¹⁴ G. Tersimonov,³ S. Thakur,⁴ D. Thomas,¹⁰⁸ A. Tikhonov,¹⁴⁰ A. R. Timmins,¹¹⁴ M. Tkacik,¹⁰⁶ T. Tkacik,¹⁰⁶ A. Toia,⁶³ R. Tokumoto,⁹² N. Topilskaya,¹⁴⁰ M. Toppi,⁴⁸ F. Torres-Acosta,¹⁸ T. Tork,⁷² A. G. Torres Ramos,³¹ A. Trifiró,^{30,52} A. S. Triolo,^{30,52} S. Tripathy,⁵⁰ T. Tripathy,⁴⁶ S. Trogolo,³² V. Trubnikov,³ W. H. Trzaska,¹¹⁵ T. P. Trzcinski,¹³³ A. Tumkin,¹⁴⁰ R. Turrisi,⁵³ T. S. Tveter,¹⁹ K. Ullaland,²⁰ B. Ulukutlu,⁹⁵ A. Uras,¹²⁶ M. Urioni,^{54,131} G. L. Usai,²² M. Vala,³⁷ N. Valle,²¹ L. V. R. van Doremalen,⁵⁸ M. van Leeuwen,⁸⁴ C. A. van Veen,⁹⁴ R. J. G. van Weelden,⁸⁴ P. Vande Vyvre,³² D. Varga,¹³⁶ Z. Varga,¹³⁶ M. Vasileiou,⁷⁸ A. Vasiliev,¹⁴⁰ O. Vázquez Doce,⁴⁸ V. Vechernin,¹⁴⁰ E. Vercellin,²⁴ S. Vergara Limón,⁴⁴ L. Vermunt,⁹⁷ R. Vértesi,¹³⁶ M. Verweij,⁵⁸ L. Vickovic,³³ Z. Vilakazi,¹²¹ O. Villalobos Baillie,¹⁰⁰ G. Vino,⁴⁹ A. Vinogradov,¹⁴⁰ T. Virgili,²⁸ V. Vislavicius,⁸³ A. Vodopyanov,¹⁴¹ B. Volkel,³² M. A. Völkl,⁹⁴ K. Voloshin,¹⁴⁰ S. A. Voloshin,¹³⁴ G. Volpe,³¹ B. von Haller,³² I. Vorobyev,⁹⁵ N. Vozniuk,¹⁴⁰ J. Vrláková,³⁷ C. Wang,³⁹ D. Wang,³⁹ Y. Wang,³⁹ A. Wegrzynek,³² F. T. Weiglhofer,³⁸ S. C. Wenzel,³² J. P. Wessels,¹³⁵ S. L. Weyhmler,¹³⁷ J. Wiechula,⁶³ J. Wikne,¹⁹ G. Wilk,⁷⁹ J. Wilkinson,⁹⁷ G. A. Willems,¹³⁵ B. Windelband,⁹⁴ M. Winn,¹²⁸ J. R. Wright,¹⁰⁸ W. Wu,³⁹ Y. Wu,¹¹⁸ R. Xu,⁶ A. Yadav,⁴² A. K. Yadav,¹³² S. Yalcin,⁷¹ Y. Yamaguchi,⁹² K. Yamakawa,⁹² S. Yang,²⁰ S. Yano,⁹² Z. Yin,⁶ I.-K. Yoo,¹⁶ J. H. Yoon,⁵⁷ S. Yuan,²⁰ A. Yuncu,⁹⁴ V. Zaccolo,²³ C. Zampolli,³² F. Zanone,⁹⁴ N. Zardoshti,^{32,100} A. Zarochentsev,¹⁴⁰ P. Závada,⁶¹ N. Zaviyalov,¹⁴⁰ M. Zhalov,¹⁴⁰ B. Zhang,⁶ L. Zhang,³⁹ S. Zhang,³⁹ X. Zhang,⁶ Y. Zhang,¹¹⁸ Z. Zhang,⁶ M. Zhao,¹⁰ V. Zherebchevskii,¹⁴⁰ Y. Zhi,¹⁰ D. Zhou,⁶ Y. Zhou,⁸³ J. Zhu,^{6,97} Y. Zhu,⁶ S. C. Zugravel,⁵⁵ and N. Zurlo^{131,54}

(ALICE Collaboration)

¹A.I. Alikhanyan National Science Laboratory (Yerevan Physics Institute) Foundation, Yerevan, Armenia

²AGH University of Science and Technology, Cracow, Poland

³Bogolyubov Institute for Theoretical Physics, National Academy of Sciences of Ukraine, Kiev, Ukraine

⁴Bose Institute, Department of Physics, and Centre for Astroparticle Physics and Space Science (CAPSS), Kolkata, India

⁵California Polytechnic State University, San Luis Obispo, California, USA

⁶Central China Normal University, Wuhan, China

⁷Centro de Aplicaciones Tecnológicas y Desarrollo Nuclear (CEADEN), Havana, Cuba

⁸Centro de Investigación y de Estudios Avanzados (CINVESTAV), Mexico City and Merida, Mexico

⁹Chicago State University, Chicago, Illinois, USA

¹⁰China Institute of Atomic Energy, Beijing, China

¹¹Chungbuk National University, Cheongju, Republic of Korea

¹²Comenius University Bratislava, Faculty of Mathematics, Physics and Informatics, Bratislava, Slovak Republic

¹³COMSATS University Islamabad, Islamabad, Pakistan

- ¹⁴Creighton University, Omaha, Nebraska, USA
- ¹⁵Department of Physics, Aligarh Muslim University, Aligarh, India
- ¹⁶Department of Physics, Pusan National University, Pusan, Republic of Korea
- ¹⁷Department of Physics, Sejong University, Seoul, Republic of Korea
- ¹⁸Department of Physics, University of California, Berkeley, California, USA
- ¹⁹Department of Physics, University of Oslo, Oslo, Norway
- ²⁰Department of Physics and Technology, University of Bergen, Bergen, Norway
- ²¹Dipartimento di Fisica, Università di Pavia, Pavia, Italy
- ²²Dipartimento di Fisica dell'Università and Sezione INFN, Cagliari, Italy
- ²³Dipartimento di Fisica dell'Università and Sezione INFN, Trieste, Italy
- ²⁴Dipartimento di Fisica dell'Università and Sezione INFN, Turin, Italy
- ²⁵Dipartimento di Fisica e Astronomia dell'Università and Sezione INFN, Bologna, Italy
- ²⁶Dipartimento di Fisica e Astronomia dell'Università and Sezione INFN, Catania, Italy
- ²⁷Dipartimento di Fisica e Astronomia dell'Università and Sezione INFN, Padova, Italy
- ²⁸Dipartimento di Fisica 'E.R. Caianiello' dell'Università and Gruppo Collegato INFN, Salerno, Italy
- ²⁹Dipartimento DISAT del Politecnico and Sezione INFN, Turin, Italy
- ³⁰Dipartimento di Scienze MIFT, Università di Messina, Messina, Italy
- ³¹Dipartimento Interateneo di Fisica 'M. Merlin' and Sezione INFN, Bari, Italy
- ³²European Organization for Nuclear Research (CERN), Geneva, Switzerland
- ³³Faculty of Electrical Engineering, Mechanical Engineering and Naval Architecture, University of Split, Split, Croatia
- ³⁴Faculty of Engineering and Science, Western Norway University of Applied Sciences, Bergen, Norway
- ³⁵Faculty of Nuclear Sciences and Physical Engineering, Czech Technical University in Prague, Prague, Czech Republic
- ³⁶Faculty of Physics, Sofia University, Sofia, Bulgaria
- ³⁷Faculty of Science, P.J. Šafárik University, Košice, Slovak Republic
- ³⁸Frankfurt Institute for Advanced Studies, Johann Wolfgang Goethe-Universität Frankfurt, Frankfurt, Germany
- ³⁹Fudan University, Shanghai, China
- ⁴⁰Gangneung-Wonju National University, Gangneung, Republic of Korea
- ⁴¹Gauhati University, Department of Physics, Guwahati, India
- ⁴²Helmholtz-Institut für Strahlen- und Kernphysik, Rheinische Friedrich-Wilhelms-Universität Bonn, Bonn, Germany
- ⁴³Helsinki Institute of Physics (HIP), Helsinki, Finland
- ⁴⁴High Energy Physics Group, Universidad Autónoma de Puebla, Puebla, Mexico
- ⁴⁵Horia Hulubei National Institute of Physics and Nuclear Engineering, Bucharest, Romania
- ⁴⁶Indian Institute of Technology Bombay (IIT), Mumbai, India
- ⁴⁷Indian Institute of Technology Indore, Indore, India
- ⁴⁸INFN, Laboratori Nazionali di Frascati, Frascati, Italy
- ⁴⁹INFN, Sezione di Bari, Bari, Italy
- ⁵⁰INFN, Sezione di Bologna, Bologna, Italy
- ⁵¹INFN, Sezione di Cagliari, Cagliari, Italy
- ⁵²INFN, Sezione di Catania, Catania, Italy
- ⁵³INFN, Sezione di Padova, Padova, Italy
- ⁵⁴INFN, Sezione di Pavia, Pavia, Italy
- ⁵⁵INFN, Sezione di Torino, Turin, Italy
- ⁵⁶INFN, Sezione di Trieste, Trieste, Italy
- ⁵⁷Inha University, Incheon, Republic of Korea
- ⁵⁸Institute for Gravitational and Subatomic Physics (GRASP), Utrecht University/Nikhef, Utrecht, Netherlands
- ⁵⁹Institute of Experimental Physics, Slovak Academy of Sciences, Košice, Slovak Republic
- ⁶⁰Institute of Physics, Homi Bhabha National Institute, Bhubaneswar, India
- ⁶¹Institute of Physics of the Czech Academy of Sciences, Prague, Czech Republic
- ⁶²Institute of Space Science (ISS), Bucharest, Romania
- ⁶³Institut für Kernphysik, Johann Wolfgang Goethe-Universität Frankfurt, Frankfurt, Germany
- ⁶⁴Instituto de Ciencias Nucleares, Universidad Nacional Autónoma de México, Mexico City, Mexico
- ⁶⁵Instituto de Física, Universidade Federal do Rio Grande do Sul (UFRGS), Porto Alegre, Brazil
- ⁶⁶Instituto de Física, Universidad Nacional Autónoma de México, Mexico City, Mexico
- ⁶⁷iThemba LABS, National Research Foundation, Somerset West, South Africa
- ⁶⁸Jeonbuk National University, Jeonju, Republic of Korea
- ⁶⁹Johann-Wolfgang-Goethe Universität Frankfurt Institut für Informatik, Fachbereich Informatik und Mathematik, Frankfurt, Germany
- ⁷⁰Korea Institute of Science and Technology Information, Daejeon, Republic of Korea
- ⁷¹KTO Karatay University, Konya, Turkey
- ⁷²Laboratoire de Physique des 2 Infinis, Irène Joliot-Curie, Orsay, France

- ⁷³Laboratoire de Physique Subatomique et de Cosmologie, Université Grenoble-Alpes, CNRS-IN2P3, Grenoble, France
- ⁷⁴Lawrence Berkeley National Laboratory, Berkeley, California, USA
- ⁷⁵Lund University Department of Physics, Division of Particle Physics, Lund, Sweden
- ⁷⁶Nagasaki Institute of Applied Science, Nagasaki, Japan
- ⁷⁷Nara Women's University (NWU), Nara, Japan
- ⁷⁸National and Kapodistrian University of Athens, School of Science, Department of Physics, Athens, Greece
- ⁷⁹National Centre for Nuclear Research, Warsaw, Poland
- ⁸⁰National Institute of Science Education and Research, Homi Bhabha National Institute, Jatni, India
- ⁸¹National Nuclear Research Center, Baku, Azerbaijan
- ⁸²National Research and Innovation Agency - BRIN, Jakarta, Indonesia
- ⁸³Niels Bohr Institute, University of Copenhagen, Copenhagen, Denmark
- ⁸⁴Nikhef, National institute for subatomic physics, Amsterdam, Netherlands
- ⁸⁵Nuclear Physics Group, STFC Daresbury Laboratory, Daresbury, United Kingdom
- ⁸⁶Nuclear Physics Institute of the Czech Academy of Sciences, Husinec-Řež, Czech Republic
- ⁸⁷Oak Ridge National Laboratory, Oak Ridge, Tennessee, USA
- ⁸⁸Ohio State University, Columbus, Ohio, USA
- ⁸⁹Physics department, Faculty of science, University of Zagreb, Zagreb, Croatia
- ⁹⁰Physics Department, Panjab University, Chandigarh, India
- ⁹¹Physics Department, University of Jammu, Jammu, India
- ⁹²Physics Program and International Institute for Sustainability with Knotted Chiral Meta Matter (SKCM2), Hiroshima University, Hiroshima, Japan
- ⁹³Physikalisches Institut, Eberhard-Karls-Universität Tübingen, Tübingen, Germany
- ⁹⁴Physikalisches Institut, Ruprecht-Karls-Universität Heidelberg, Heidelberg, Germany
- ⁹⁵Physik Department, Technische Universität München, Munich, Germany
- ⁹⁶Politecnico di Bari and Sezione INFN, Bari, Italy
- ⁹⁷Research Division and ExtreMe Matter Institute EMMI, GSI Helmholtzzentrum für Schwerionenforschung GmbH, Darmstadt, Germany
- ⁹⁸Saga University, Saga, Japan
- ⁹⁹Saha Institute of Nuclear Physics, Homi Bhabha National Institute, Kolkata, India
- ¹⁰⁰School of Physics and Astronomy, University of Birmingham, Birmingham, United Kingdom
- ¹⁰¹Sección Física, Departamento de Ciencias, Pontificia Universidad Católica del Perú, Lima, Peru
- ¹⁰²Stefan Meyer Institut für Subatomare Physik (SMI), Vienna, Austria
- ¹⁰³SUBATECH, IMT Atlantique, Nantes Université, CNRS-IN2P3, Nantes, France
- ¹⁰⁴Sungkyunkwan University, Suwon City, Republic of Korea
- ¹⁰⁵Suranaree University of Technology, Nakhon Ratchasima, Thailand
- ¹⁰⁶Technical University of Košice, Košice, Slovak Republic
- ¹⁰⁷The Henryk Niewodniczanski Institute of Nuclear Physics, Polish Academy of Sciences, Cracow, Poland
- ¹⁰⁸The University of Texas at Austin, Austin, Texas, USA
- ¹⁰⁹Universidad Autónoma de Sinaloa, Culiacan, Mexico
- ¹¹⁰Universidade de São Paulo (USP), São Paulo, Brazil
- ¹¹¹Universidade Estadual de Campinas (UNICAMP), Campinas, Brazil
- ¹¹²Universidade Federal do ABC, Santo Andre, Brazil
- ¹¹³University of Cape Town, Cape Town, South Africa
- ¹¹⁴University of Houston, Houston, Texas, USA
- ¹¹⁵University of Jyväskylä, Jyväskylä, Finland
- ¹¹⁶University of Kansas, Lawrence, Kansas, USA
- ¹¹⁷University of Liverpool, Liverpool, United Kingdom
- ¹¹⁸University of Science and Technology of China, Hefei, China
- ¹¹⁹University of South-Eastern Norway, Kongsberg, Norway
- ¹²⁰University of Tennessee, Knoxville, Tennessee, USA
- ¹²¹University of the Witwatersrand, Johannesburg, South Africa
- ¹²²University of Tokyo, Tokyo, Japan
- ¹²³University of Tsukuba, Tsukuba, Japan
- ¹²⁴University Politehnica of Bucharest, Bucharest, Romania
- ¹²⁵Université Clermont Auvergne, CNRS/IN2P3, LPC, Clermont-Ferrand, France
- ¹²⁶Université de Lyon, CNRS/IN2P3, Institut de Physique des 2 Infinis de Lyon, Lyon, France
- ¹²⁷Université de Strasbourg, CNRS, IPHC UMR 7178, F-67000 Strasbourg, France, Strasbourg, France
- ¹²⁸Université Paris-Saclay Centre d'Etudes de Saclay (CEA), IRFU, Département de Physique Nucléaire (DPhN), Saclay, France
- ¹²⁹Università degli Studi di Foggia, Foggia, Italy

¹³⁰*Università del Piemonte Orientale, Vercelli, Italy*

¹³¹*Università di Brescia, Brescia, Italy*

¹³²*Variable Energy Cyclotron Centre, Homi Bhabha National Institute, Kolkata, India*

¹³³*Warsaw University of Technology, Warsaw, Poland*

¹³⁴*Wayne State University, Detroit, Michigan, USA*

¹³⁵*Westfälische Wilhelms-Universität Münster, Institut für Kernphysik, Munster, Germany*

¹³⁶*Wigner Research Centre for Physics, Budapest, Hungary*

¹³⁷*Yale University, New Haven, Connecticut, USA*

¹³⁸*Yonsei University, Seoul, Republic of Korea*

¹³⁹*Zentrum für Technologie und Transfer (ZTT), Worms, Germany*

¹⁴⁰*Affiliated with an institute covered by a cooperation agreement with CERN*

¹⁴¹*Affiliated with an international laboratory covered by a cooperation agreement with CERN*

^aDeceased.

^bAlso at: Max-Planck-Institut für Physik, Munich, Germany.

^cAlso at: Italian National Agency for New Technologies, Energy and Sustainable Economic Development (ENEA), Bologna, Italy.

^dAlso at: Dipartimento DET del Politecnico di Torino, Turin, Italy.

^eAlso at: Department of Applied Physics, Aligarh Muslim University, Aligarh, India.

^fAlso at: Institute of Theoretical Physics, University of Wrocław, Poland.

^gAlso at: An institution covered by a cooperation agreement with CERN.